Exploring Phage-*Staphylococcus aureus* Host Dynamics Through Innovative *In Vitro* Experiment and Pharmacokinetic/pharmacodynamic Modeling

Kévin Royet[1,4], Leslie Blazere[1], Emilie Helluin[1], Ludivine Coignet[1], Lucile Plumet[7], Mélanie Bonhomme[1], Camille Kolenda[1,2], Romain Garreau[4,5,6], Florent Valour[1,3], Mathieu Médina[1], Frédéric Laurent[1,2], Sylvain Goutelle[* 4,5,6]

[1]CIRI - Centre International de Recherche en Infectiologie, Inserm, U1111, Université Claude Bernard Lyon 1, CNRS, UMR5308, Ecole Normale Supérieure de Lyon, Univ Lyon, F-69007, Lyon, France

[2]Service des maladies infectieuses et tropicales, Hospices Civils de Lyon, Lyon, France

[3]Laboratoire de Bactériologie, Institut des Agents Infectieux, French National Reference Centre for Staphylococci, Hospices Civils de Lyon, Lyon, France

[4] Univ Lyon, Université Claude Bernard Lyon 1, UMR CNRS 5558, Laboratoire de Biométrie et Biologie Évolutive, Villeurbanne, France.

[5] Univ Lyon, Université Claude Bernard Lyon 1, Faculté de Pharmacie de Lyon, Lyon, France

[6] Hospices Civils de Lyon, Groupement Hospitalier Nord, Service de Pharmacie, Lyon, France

[7] Laboratory of Pathogen Host Interactions, Université de Montpellier, CNRS, UMR 5235, Montpellier, France

***Corresponding author:** Sylvain Goutelle, Laboratoire de Biométrie et Biologie évolutive, Université Claude Bernard Lyon 1, CNRS, UMR5558, 43 boulevard du 11 Novembre 1918, Lyon, France. E-mail address: sylvain.goutelle@univ-lyon1.fr.

Abstract

Phage therapy is considered a potential alternative/adjuvant to antibiotics for treating multidrug resistant infections. The clinical implementation of phage therapy is challenging for various reasons, including knowledge gaps in bacteria/phage interactions, particularly the phage's self-replication within its bacterial host. Here, we combine *in vitro* experiments and modeling approaches to explore kinetic between *S. aureus* and a promising therapeutic phage from our collection. We demonstrate the emergence of a phage-insensitive population, whose final concentration and growth constant is phage dose dependent. Free phages, sensitive bacteria, non-sensitive bacteria and infected bacteria integrate a 4 differential equations model that fits well with time series data. Inundation and proliferation thresholds, as well as rate constants are thus calculated. Results predict that the phage dose used could be critical, with the strange likelihood that higher doses used are less effective. The use and adaptation of this model to specific systems can guide experimental design. Altogether, our results illustrate how such *in vitro* studies are an essential precursor to understand the kinetic properties of future *in vivo* experiments.

Introduction

The emergence of antibiotic resistance is one of the major public health threats requiring a multidisciplinary and global approach to health issues, known as One Health [1]. While development of new antibiotics is still of interest, alternative or complementary therapeutic strategies are necessary. Therapy using bacteriophages (or phages) is the source of considerable hope [2], [3]. Phage therapy has been developed and used for decades In Western countries, where it is considered that clinical evidence is currently not sufficient to be approved by health authorities. In those countries, phage therapy is only used as compassionate basis when conventional treatments are ineffective. However, phage therapy is promising and was reported to be life-saving in several cases [4].

Phages do not have approval for marketing in either Europe or the United States, partly due to scarcity of available pharmacokinetic and pharmacodynamic (PK/PD) data [5]. The PK/PD of phages is very different from that of antibiotics and more complex since phages have the ability to self-replicate in the presence of their target bacteria [6]. The co-dynamics of phage and bacteria population is characterized by specific thresholds effects. The proliferation threshold is that cell density above which the probability of a progeny phage replicating is greater than the probability of that phage being lost [7]. The inundation threshold is the phage density above which the probability of a bacterial cell being lysed by a phage is greater than the probability of that same bacterial cell dividing [6]. Quantifying those thresholds for a given phage-bacteria pair is important to design dosage regimen.

S. aureus is responsible for various infections, including bacteremia, sepsis, pneumonia, endocarditis and bone and joint infections (BJI). Resistance of *S. aureus* to antibiotics is widespread, a clinically relevant entity being methicillin resistant strains [8]. Because of its ability to form biofilms, this pathogen is also difficult to eradicate in device-associated infections. For those reasons, *S. aureus* is classified as high priority for R&D of new therapeutics by the WHO and is a target of interest for the development of phage therapy [9].

The objectives of this study were i. to describe and quantify *in vitro* co-dynamic of three candidate antistaphylococcal phages (V1SA019, V1SA020 and V1SA022) isolated during PHAG-ONE project (project reference: 20-AMRA-0009) and their SH1000 or USA300 *S. aureus* bacterial targets; and ii. to build a robust mathematical model describing these co-dynamics.

Materials and methods

Experimental method

Culture and count of *S. aureus* and bacteriophages

We used two strains of *S. aureus* in our experiments, SH1000 [10] and USA300 LAC strain [11], as well as three phage candidates, V1SA019, V1SA020 or V1SA022 (Hospices civils de Lyon).

S. aureus strains were weekly grown on Columbia Agar supplemented with 5% Sheep Blood (BioMerieux, France, manufacturer's reference: 43041) for 20 hours at 37 °C. For culture, one colony was pricked with an oese and suspended in cation adjusted Mueller Hinton (caMH) (Becton Dickinson, Franklin Lakes, NJ, USA), then incubated at 37 °C for 20 hours at 180rpm. *S. aureus* was counted using agar caMH (BioRad, Hercules, USA). *S. aureus* bacteriophage V1SA019, V1SA020 or V1SA022 (Hospices civils de Lyon) were routinely propagated and counted on strain P2SA225 or P2SA237 when appropriate, *S. aureus* prophage free strains (Staphyloccocal reference center, Lyon, France), via spot test or double layer plaque assay performed with caMH.

In vitro time-kill experiments

Four series of time-kill experiments were conducted. The effect of the three phages (V1SA019, V1SA020 or V1SA022) was evaluated on *S. aureus* SH100 strain. In addition, V1SA19 was also evaluated on *S. aureus* USA300 LAC strain. This permitted to study the variability of the phage-bacteria dynamics between phages and between bacterial strains.

S. aureus SH1000 or USA300 strains were grown in cation adjusted Mueller Hinton (caMH) culture medium (Becton Dickinson). After 16h at 37 °C, OD_{600} was measured and an aliquot was added to 25mL pre-warmed caMH in conical tube (Falcon, Le Pont de Claix, France, 50mL) to a final concentration of 3 log_{10} colony-forming units (CFU) mL^{-1} and incubated at 37°C under microaerobic condition with shaking at 180 rpm. At 1h post inoculation, bacteriophage V1SA019, V1SA020 or V1SA022 were added to a final concentration of 1 log_{10} plaque-forming units (PFU) mL^{-1}, 3 log_{10} PFU mL^{-1} or 5 log_{10} PFU mL^{-1} to give approximate multiplicity of infection (MOI) of 0.01, 1, 100. Samples were taken every 2 hours for 24 hours. Each aliquot was serially diluted and *S. aureus* count were performed by spot test. After 8 hours of kinetic, 250uL of samples were also spread on caMH agar to detect down to 4 CFU mL^{-1}. Each aliquot was then centrifuged 30s at 20.000g to remove *S. aureus*

cells and supernatant was diluted for bacteriophages enumeration by spot test or double layer plaque assays when applicable (when estimated PFU mL^{-1} < 2,2 log_{10}). At the end of the experiment, 1mL of culture was stored at -80°C in 20% glycerol allowing subsequent isolation of clones. Experiments were performed using 3 different phage production batches infecting 3 independent bacterial cultures for each MOI. All experiments were conducted in triplicates on different weeks.

Adsorption time and One-Step-Growth-Curve (burst size)

To assess the phage adsorption time, *S. aureus* SH1000 or USA300 strains were grown and inoculated into 25 mL of caMH in 50 mL conical tube (Falcon, Le Pont de Claix, France). The triplicate cultures were grown to late log phase, approximately 8 log_{10} CFU mL^{-1}, then phage was added to an approximate MOI of 0.01 and incubated at 37°C without agitation. Samples of the cultures were taken every 4 minutes up to 45 min post phage addition. Samples were passed through a 0.2 µm filter (Merk, Darmstadt, Germany) to remove *S. aureus* cells and bound phages. Unbound 'free' phages were counted using spot test and double layer plaque assays. To estimate the latent period and burst size of a single round of phage replication, the same protocol was applied with modifications: culture was serial diluted in pre-warmed caMH at 1/100, 1/1000 and 1/10000 (v/v) at "T=time of maximal adsorption" according to Kropinski and colleagues [12]. Samples of the cultures were taken every 6 minutes up to 2 hours post phage addition. For a given time, the concentration of the most diluted flask was used to avoid re-adsorption phenomena. Burst size value was calculated as follow: "Average phage concentration at plateau/Number adsorbed phage at T= time of maximal adsorption " [12]. The One-step-growth-curve experiment was carried out by 3 different operators on 3 different days, including a total of 6 independent experiments with 3 different phage production batches.

Bacteriophage decay

To determine the rate of decay of free phages in the absence of bacteria, V1SA019, V1SA020 or V1SA022 were added to 25 mL of pre-warmed caMH in 50 mL conical tube (Falcon, Le Pont de Claix, France) at a final concentration of 1 log_{10} plaque-forming units (PFU) mL^{-1}, 3 log_{10} PFU mL^{-1} or 5 log_{10} PFU mL^{-1} and incubated at 37 °C under microaerobic conditions with shaking at 180 rpm. Samples were taken for up to 48 hrs and bacteriophages enumerated via double layer plaque assay. A total of 3 independent experiments were performed.

Phage susceptibility test

From *S. aureus* clones isolated and grown 24 hrs at 37 °C on COS medium, half a colony was resuspended in a 96-well plate containing 200 µL of caMH alone or supplemented with 10^6 PFU mL^{-1} of appropriate phage. Plates were incubated at 37 °C using LogPhase 600 (Agilent BioTek, Santa Clara, USA), and OD_{600} measurements were taken every hour for 24 hrs. A clone was considered resistant when its OD_{600} exceeded 0.1 after 24 hrs of growth compared to the negative control consisting of inoculation of wild-type SH1000 in the presence of the phage.

DNA extraction and sequencing

Bacterial DNA was extracted using the Maxwell® RSC Blood DNA kit (Promega, Madison, WI, USA), after an initial incubation with 40 µg lysostaphin (Sigma-Aldrich, Saint Louis, MO, USA Aldrich), 200 µg lysozyme (Sigma-Aldrich) and 200 µg RNaseA (Qiagen, Hilden, Germany) for 1 hr at 37 °C, followed by incubation with 12 mAU (AU= Anson unit) of proteinase K (Promega) for 20 min at 60 °C. Whole genome sequencing was performed with Novaseq instrument (Illumina, San Diego, CA, USA) using a 150 bp paired-end protocol. Genome assemblies was performed using SPAdes v3.14 [11]. Prokka v1.14.5 was used for genome annotation [13].

Statistical analysis of experimental data

Statistical analyses and plotting were performed using GraphPad Prism, version 8.0.0 (GraphPad Software, San Diego, CA, USA). Variables were compared using the nonparametric Mann-Whitney U test. A p-value < 0.05 was considered significant.

PK/PD modeling

We used a population approach and nonlinear mixed effect modeling to describe the time course of bacteria and phage counts in all four sets of the experiments. All time-kill data were analyzed, as well as bacteria growth control and phage decay data. Adsorption and burst-size data could not be included in the final model, as preliminary runs showed model instability and unrealistic estimates.

A model written in ordinary differential equations (ODE) was implemented in the Monolix software (version 2024, Lixoft, Antony, France) to describe the interactions between four populations: susceptible bacteria (S), bacteria with reduced susceptibility to phages (denoted as resistant, R, for

the sake of simplicity), bacteria infected by phages (I) and free phage viruses (V). The ordinary differential equations corresponding to this model were as follows (Equation 1):

$$dS/dt = alpha*(1 - S/Bmax)*S - mut*S - bind_S*S*V$$

$$dR/dt = alpha*(1 - R/Bmax)*R + mut*S - bind_R*R*V$$

$$dI/dt = bind_S*S*V + bind_R*R*V - Lysis*I$$

$$dV/dt = burst*Lysis*I - bind_S*S*V - bind_R*R*V – decay*V$$

The eight parameters were: alpha, bacterial growth constant; Bmax, maximal concentration of bacteria; mut, mutation rate of S to R bacteria; $bind_S$ and $bind_R$, binding rate constant of phages to S and R bacteria, respectively; Lysis, lysis rate constant of I bacteria, burst; number of free phages released upon I bacteria burst; decay, elimination rate constant of free phages

This model was inspired by previously published *in vitro* PK/PD studies [14], [15]. It is shown schematically in Figure 1. The inclusion of bacteria with reduced susceptibility was necessary to describe bacterial regrowth observed in the experiments. For each parameter, both fixed (median, typical value) and random (inter-experiment variability) effect parameters were estimated, within a general framework as follows:

$$\theta_i = TV(\theta) \times exp(\eta_i) \qquad \text{Equation 2}$$

With

$$\eta_i \sim N(0, \omega^2) \qquad \text{Equation 3}$$

Where θi is the parameter value (e.g., bacteria growth rate, phage decay…) for an individual experiment, TV(θ) is the typical parameter value in the whole set of experiments, i.e. the median for a lognormal distribution (considered as a fixed effect in the nonlinear mixed effects model), and η_i is a random effect variable quantifying the variability around the typical value. Random effects were assumed to follow a normal distribution with mean of zero and variance ω^2. As a result of Equation 2, parameters (θ_i) are assumed to follow a log-normal distribution.

Model outputs were coded as $\log_{10}(S + R + I)$ and $\log_{10}(V)$ for bacteria and virus, respectively, to facilitate comparison with observations. Several residual error models were evaluated, including additive, proportional and combined error models, on the log scale. Phage production batch was evaluated as a potential descriptor of inter-experiment variability.

Model evaluation was based on goodness-of-fit criteria including objective function (-2*log-likelihood) and Akaike Information Criterion (AIC). Plots of observed versus model individual estimates were examined, as well as distributions of individual weighted residuals. Visual predictive checks based on 1000 simulations were performed as internal validation. Because proliferation and inundation thresholds are not primary parameters but combination of ODE parameters [15], they were not estimated at the population level but computed for each experiment after Bayesian estimation of individual parameters and summarized with descriptive statistics.

The proliferation thresholds of phages for susceptible and resistant bacteria ($Prolif_S$ and $Prolif_R$) were calculated as follows [15] :

$$Prolif_S = \frac{dec}{bind_S \times (burst - 1)} \qquad \text{Equation 4}$$

$$Prolif_R = \frac{dec}{bind_R \times (burst - 1)} \qquad \text{Equation 5}$$

The inundations thresholds for susceptible and resistant bacteria ($Inund_S$ and $Inund_R$) were calculated as follows [15]:

$$Inund_S = \frac{alpha - mut}{bind_S} \qquad \text{Equation 6}$$

$$Inund_R = \frac{alpha}{bind_R} \qquad \text{Equation 7}$$

Finally, simulations were performed based on the final model for V1SA019 / SH1000 to study the influence of phage dose size on antibacterial effect.

Results

Adsorption, burst size and decay

Adsorption assays showed a clear decline in free phages due to phage attachment to sensitive bacteria, reaching a plateau after 24 min, 32 min or 24 min (named maximum adsorption time thereafter) where a maximum of 99.9 %, 97 % and 95 % of V1SA019, V1SA020 and V1SA022 phages attached to SH1000 respectively. A plateau was reached after 32 min during adsorption assay conducted with V1SA019 and USA300 with a maximum of 99,5 % of attached phages (Figure 2). Adsorption times, defined as the time where >90% of phages are adsorbed to bacteria, were 8, 20, 16 min for V1SA019, V1SA020, and V1SA022, respectively with SH1000 and 8 min for V1SA019 with USA300 (Table S1).

During One Step Growth curve experiments, a latent phase of 24, 24 and 32 min was observed for V1SA019, V1SA020, V1SA022 on SH1000 respectively and of 6 min for V1SA019 on USA300. This was followed by a release phase, until a plateau was reached at approximately 1.5-2 hrs (Figure 3). Estimated median burst sizes were 42, 24 and 27 for V1SA019, V1SA020 and V1SA022 on SH1000 and 134 for V1SA019 on USA300. (Table S2).

In absence of bacteria, phages declined in a linear manner on the log-scale (Figure 4). The loss of phage viability over 24 hours was low for each phage (mean ratio < 10 PFU.mL^{-1} between 0-24 hrs) for all the concentrations tested, although significant for inoculum values of 1 $\log_{10}$ PFU mL^{-1} and 5 $\log_{10}$ PFU mL^{-1} of V1SA019, V1SA020 and V1SA022. Over 48 hours, the loss of phage viability was larger, with mean ratios of 5.4, 3.6, 3.2 for V1SA019; 7, 27, 39 for V1SA020; 9, 34, 43 for V1SA022 for inoculum of 1 $\log_{10}$ PFU.mL^{-1}, 3 $\log_{10}$ PFU.mL^{-1} and 5 $\log_{10}$ PFU.mL^{-1}, respectively.

In vitro time-kill studies

Phage-bacteria kinetic experiments were conducted at MOI of 0.01, 1, 100. Figure 5 shows a scatter plot of pooled results of bacteria and phage counts and indicates a regular pattern: exponential growth of bacteria was followed by rapid proliferation of phages, then the bacterial population collapsed between 6 and 10 h, while the phage population reached a plateau. An exception to this regular pattern was observed for experiments conducted with V1SA019 on USA300 at MOI of 0.01 where bacterial collapse was observed later, after about 18-20 hours and slight decline of phage population was visible at 10-12 hours. In several experiments, a regrowth of bacteria was observed, suggesting non-susceptibility to phage. The slope of regrowth appeared to increase with increasing MOI, which was confirmed by the modeling (see below). The final phage concentration was about 9-11 $\log_{10}$ PFU.mL^{-1} depending on the phage/bacteria couple considered, irrespective of MOI. A slight decline of phage plateau was visible for V1SA019 on SH1000, especially for MOI of 100.

Population PK/PD modeling

The *S. aureus* SH1000 / phage V1SA019 pair is used as an illustration for the PK/PD modeling in the manuscript, while results for the other bacteria/phage pairs are provided as supplementary material.

The four-equation, eight-parameter model fitted individual bacteria and phages data very well, as shown in Figure 6 for the V1SA019 / SH1000 pair, and supplementary Figure S1 for the other pairs. Model parameters are shown in

Table **1** for the SH1000 / V1SA019 pair and summarized in supplementary Table S3 for all experiments. Phage production batch showed no influence on PK/PD parameters in all four models. They were minor differences in the final model between the four experiments, regarding Bmax parameter (fixed for V1SA019 / SH1000, random for the other pairs) and error model. Overall, most parameters were estimated with acceptable precision (relative standard error < 50%), including inter-experiment variability. Large imprecision was observed for the median mutation rate (except for V1SA019 / SH1000 pairs). This was likely due to the high interexperiment variability of this parameter (high omega values). A common feature between the four models was a phage binding rate of R bacteria ($bind_R$) lower than that for S bacteria ($bind_S$), resulting in higher proliferation and inundation thresholds for R compared to S bacteria. Also, the estimated typical burst size was larger than the values directly estimated from experimental data. By comparing results obtained with SH1000 strain for the three phage candidates (V1SA019, V1SA020, V1SA022), one can see between phages differences in mutation rate, burst size and decay. The comparison of the V1SA019 / SH1000 and V1SA019 / USA 300 model parameters also reveals differences associated with the bacteria strain. The USA 300 strain displayed a 10-fold lower median burst size and much lower median mutation rate, compared with the SH1000 strain. However, considerable variability was observed for the mutation rate for the V1SA019 / USA 300 experiments, with values ranging from 0 to 5.25×10^{-8} between experiments (median = 1.26×10^{-13}).

Visual predictive checks shown in

Figure **7** for V1SA019 / SH1000 supported internal validation of the model. Those plots also exhibited different patterns of bacterial dynamics, including a sharp decline followed by regrowth of total bacteria count after 10-12h, with variable slopes. Another pattern of constant growth up to a maximum value corresponded to control experiments conducted with bacteria only (no phage).

The model also well described the time-course of the bacteria and phage counts of individual experiments. A selection of individual fits for various initial MOI is shown in Figure S3 for our reference pair V1SA019 / SH1000. Those plots illustrate the bacterial regrowth that appeared to increase with increasing phage dose.

This was confirmed by simulations performed with the final model parameters for various phage doses, shown in Figure 8. While regrowth was generally limited for initial MOI of 0.01, it was dramatic

for initial MOI of 1 and 100. The slope of bacterial regrowth appeared to be dependent on the initial phage concentration. Such regrowth was driven by emergence of the bacterial population with reduced susceptibility to phages. However, a phage dose above the inundation threshold (1.10^{10} PFU/mL) resulted in very fast killing of all bacteria and no regrowth according to simulations.

Emergence of a resistant bacterial subpopulation

At the end of the experiments between V1SA019 and SH1000 exclusively, one clone from each of the replicates of the three initial MOIs (i.e. three clones per MOI) was randomly selected, isolated, purified and sequenced. The resistance of these nine mutants was confirmed by spot test with phage V1SA019 as a predator, where no lysis zone was observed (data not shown). These clones were tested for fitness in caMH in comparison with the wild strain and all showed a growth defect (Data not shown). Each clone carried at least one non-synonymous mutation or partial gene deletion leading to premature stop codons. Eight genes are affected by these mutations, namely *tarA, tarK, tagO sRNA35, tsr24, znuB, rpoB* and *purR*. All mutants carried at least one mutation (non-synonymous or deletion) in one of the genes involved in the teichoic acid biosynthesis pathway, namely *tarA, tarK* or *tagO*, according to KEGG pathway (KEGG pathway database) Table S4.

The model predicted the appearance of R bacteria as early as eight hours after infection, irrespective of the initial MOI. After 8, 10, 12, 16 and 24 hrs of infection, up to 60 clones were isolated and tested for susceptibility to phage V1SA019 in liquid culture medium. At 8 hrs, 0 %, 7 % and 7 % (60, 27 and 30 clones tested) resistant clones were identified for MOI of 0.01, 1 and 100 respectively. At 10 hrs, 0 %, 0 % and 19% (60, 1 and 27 clones tested) resistant clones were identified for MOI of 0.01, 1 and 100 respectively. At 12h, 0% resistant clones were identified for MOI of 0.01 and 1 (30 and 22 clones tested) but this percentage increased up to 33% and 100% (3 and 10 clones tested) for MOI 0.01 and 1 respectively. At 24 hrs, 96 % resistant clones were identified for MOI of 0.01 and 100 % for MOI of 1 and 100 (24, 30 and 30 clones tested respectively) (Table S5).

Discussion

Co-dynamics of bacteria and phage and variability

We used in vitro experiments and mathematical modeling to study the co-dynamics of two *S. aureus* strains and three phage candidates. Briefly, phage-bacteria kinetic experiments conducted at three initial MOIs showed bacterial regrowth in the majority of cases. The slope of regrowth appeared to increase with MOI. The PK/PD modeling suggest that the emergent R subpopulation was characterized by a phage binding lower than that of S bacteria, and specific values of the proliferation and inundation thresholds.

Our analysis confirmed that the co-dynamics of phage and bacteria can be described by ODE and is driven by predator-prey interactions. Our model was inspired by that of Cairns and collaborators [15]. Such mathematical models were developed from studies performed *in silico* or in laboratory conditions on pathogens such as *Salmonella thyphimurium* or *Campylobacter jejuni* [14], [15], [16], [17], [18], [19]. Probabilistic models for predicting *S. aureus* inactivation by two phages in pasteurized milk were also previously developed based on logistic regression procedure [20]. However, to our knowledge, a model based on differential equations applied to the modeling of dynamic interaction between *S. aureus* and lytic phages in laboratory conditions had not yet been developed.

Also, we used a non-linear mixed-effects approach that allowed to quantify experimental variability in PK/PD parameters, which was substantial for some of the parameters (mutation rate, burst size).

A strength of our study is to examine three different phage candidates and two bacteria strain. Our results suggest differences in key parameters of the dynamics, especially between SH1000 and USA 300 strains. This suggests that bacteria/phage dynamics is likely specific of each pair and cannot be generalized or extrapolated from a single case study.

Proliferation and inundation thresholds

Our model allowed us to calculate inundation and proliferation thresholds that define two modes of phage therapy : passive and active respectively [7], [21]. Our in *vitro*-times kill studies show that bacteria grow in the presence of a virulent phage until the phage reaches a critical concentration, called inundation threshold, beyond which susceptible bacteria are rapidly infected and killed. Previous model provided the minimum phage concentration (about 2×10^8 PFU $ml^{-1)}$required to inactivate *S. aureus* in milk [20]. This number is very close to the inundation thresholds (for S bacteria) calculated for each of our phage/S bacteria pairs, ranging from 1 to 7 x 10^8 PFU ml-1 although the experimental conditions are different. Proliferation threshold is much more difficult to observe on time series data, as explained by Cairns in 2009, since we observed only free phages and not total phages [15]. The proliferation thresholds (for S bacteria) observed in our experiments ranged from 4.8 x 10^4 to 2.1 x 10^5 CFU/mL and appear to be independent of the initial dose of phage, the phage itself or the bacterial strain considered.

Although these thresholds may vary in other *in vitro* and *in vivo* contexts, this work shows that in the case of active therapy, a minimum bacterial quantity is necessary to allow the phage titer to increase, reach the inundation threshold and finally reduce the bacterial load [22]. This might suggest that different doses of phages, i.e. below the inundation threshold, would have similar bacterial load control kinetics, but this is not correct. Indeed, our study showed a direct impact of the initial dose of phage, where the highest dose (but lower than the inundation threshold) has an impact both on the average final quantity of resistant bacteria and on its average growth rate. This phenomenon was observed for each of the phage/bacteria pairs studied. Under certain conditions (e.g. V1SA019 on SH1000 at MOI of 0.01), an absence of R bacteria was even observed at the end of the experiment although this phenomenon appears to be random.

The correlation between bacteria regrowth and initial MOI is intriguing. Our simulations performed with various MOI provided interesting insights (Figure 8) and suggest the importance of achieving the inundation threshold of the resistant subpopulation for controlling the regrowth with active phage therapy. For the lowest MOI (0.01), it takes longer for the phage population to achieve the inundation threshold of S bacteria. This leaves more time for S bacteria to grow, and the S bacteria peak is the highest, compared with higher MOI. The phage population plateau is also higher, close to the inundation threshold of R bacteria estimated at 3.7 x 10^{10} PFU/mL (median). By contrast, higher MOI

result in lower S bacteria peak and lower phage plateau, below the inundation threshold of R bacteria. Based on those observations, we assume that two ways exist to prevent the emergence of R bacteria and prevent bacteria regrowth in such in vitro conditions. The first one is to use a very high dose of phage, greater that the inundation threshold of S bacteria that totally suppress the mutation process (passive therapy). The other option is to use active therapy with a phage dose that permits phage amplification up to the inundation threshold of R bacteria.

For doses above the inundation threshold (passive therapy), bacterial concentration will be rapidly reduced by adsorption and lysis of almost all susceptible bacterial cells. While our simulation results suggest that administration of a phage dose above the inundation threshold would be required to achieve rapid clearance without emergence of resistant bacteria, achieving such a high concentration may be difficult, because of issues related to both formulation and infection site. Moreover, passive therapy may not be total (failure to achieve 100% eradication), leaving a susceptible population for which the probability of encountering a phage has become low [23], [24]. The phage concentration at the infection site may then decrease, while the bacterial biomass may once again grow until it reaches the proliferation threshold, leaving the way open for active therapy if viable phages are still present. Obeso and colleagues observed that inactivation of *S. aureus* by phages in milk shows a certain influence of bacterial contamination on the effectiveness of phages, probably related to the bacterial proliferation threshold [20]. In contrast, Bigwood and colleagues showed that biocontrol of *Salmonella typhimurium* presents in low numbers in liquid foods is achievable, given a sufficiently high concentration of added phages, and that it is not necessary to know the concentration of pathogens to achieve this [19]. Optimal dosage must so strike a balance between immediate efficacy and long-term outcomes.

Emergence of a resistant bacterial subpopulation

Our experimental and modeling results confirm the rapid emergence of a bacterial population resistant to phages. In our work, this population was modelled as not fully resistant but less susceptible, with estimated lower median binding rate constants, and higher proliferation and inundation thresholds.

The growth of this resistant subpopulation seemed to vary with the phage doses and was faster for higher initial phage doses in the experimental data. This effect could be an artifact caused by a closed

culture medium. Delayed control of the S bacterial population at lower MOI leads to increased depletion of the culture medium, not renewed in our experiments, via extensive and prolonged S bacterial division. At low MOI, emerging R bacteria thus find themselves in a culture medium less favorable to their growth.

The model predicted that this resistant population started to rise at about 8 hours of kinetics. We were able to confirm SH1000 resistance to V1SA019 experimentally after isolating and testing several clones present at 8h, 10h, 12h and 16h post-infection. At a given time, the percentage of phage-resistant bacteria in the bacterial population was greater for the highest phage doses. This confirms the phenomenon described above where higher MOI lead to faster emergence of resistant clones. It is unlikely that a resistant population will be present at the start of the experiment, as the rate of appearance of resistant clones varies with variables such as MOI. The estimated median mutation rate (i.e $2.64.10^{-9}$ h^{-1}) is similar to other *in vitro* calculated mutation rate for *S. aureus* population (i.e from $1.e^{-08}$ h^{-1} to $5.e^{-09}$ h^{-1}) [25], [26].

All the clones isolated post 24 hrs of infection (i.e. 9 clones in total) presented mutations in genes whose products are involved in the teichoic acid biosynthesis pathway, known to be the main receptor for phages in *S. aureus*, and Gram-positive bacteria in general [27], [28]. This indicates that, despite the difference in control of the bacterial density for various MOI, phage-induced stress leads to the same bacterial adaptation for survival regardless of the quantity of phages used. However, all these clones show a growth defect when tested individually for growth in caMH, suggesting that a fitness defect could cause them to be eliminated by the host immune system as described for *in vivo* experiment with *S. aureus* and phage predator [25], [26]. Finally, we did not sequenced clones isolated in the course of kinetic, where the presence of various sub-populations cannot be excluded. Indeed, V1SA019 susceptibility tests carried out on different clones isolated at 8 hrs and 10 hrs post-infection show the presence of both susceptible and resistant clones, with the percentage of resistant clones increasing over time.

This argument in favor of the presence of different sub-populations during kinetics is supported by the fact that for some couples (i.e, V1SA019 and SH1000) phage concentration does not simply reach a peak before maintaining a plateau, but rather undergoes a slight drop after 10 hours (0.5 to 1 log). This phenomenon has already been described by Cairns and colleagues, although on a different bacterial/phage pair, suggesting that it may be a common phenomenon and not an artifactual one, as

previously suspected [15]. Other hypotheses would be the possibility that phages mutate to infect a resistant population [29], [30]. If this hypothesis is correct, the inundation threshold associated with this population should be higher than calculated, as evidenced by the absence of bacterial population control. Second hypothesis could be that a dynamic of co-existence between phages and sensitive/resistant bacterial populations takes place [31], [32]. Given these arguments, it would be worth testing the proportion of sensitive and resistant bacteria over time and then sequencing them, as well as isolating and sequencing the phages at the end of the experiment to attempt to isolate mutant populations in future works.

Although acquisition of resistance was not experimentally checked for the USA 300 LAC strain, the model result showed a considerable variability in the estimated mutation rate, with minimal value down to zero, also suggesting that a resistant subpopulation may not exist at time zero in some experiments.

Conclusion

To develop phage therapy, it is necessary to understand the dynamics of phage-bacteria interactions and characterize key PK/PD parameters of phage candidates such as proliferation and inundation thresholds. Our results confirm that predator-prey mathematical models adequately describe the co-dynamics of a phage candidate against *S. aureus*. Variability was observed in co-dynamics and model parameters between phages and bacteria strains. The ability of phage therapy to kill susceptible bacteria and control the growth of a resistant subpopulation was influenced by phage dose, with higher doses resulting in faster growth of the resistant bacteria. Proliferation and inundation threshold of both susceptible and resistant subpopulations should be considered for phage dosing. Further research is necessary to confirm those findings for *in vivo* extrapolation.

[1] K. E. Arnold *et al.*, 'The need for One Health systems-thinking approaches to understand multiscale dissemination of antimicrobial resistance', *Lancet Planet Health*, vol. 8, no. 2, pp. e124–e133, Feb. 2024, doi: 10.1016/S2542-5196(23)00278-4.

[2] J. A. G. Fortaleza, C. J. N. Ong, and R. De Jesus, 'Efficacy and clinical potential of phage therapy in treating methicillin-resistant Staphylococcus aureus (MRSA) infections: A review', *Eur J Microbiol Immunol (Bp)*, Feb. 2024, doi: 10.1556/1886.2023.00064.

[3] M. T. Moghadam *et al.*, 'Phage therapy as a glimmer of hope in the fight against the recurrence or emergence of surgical site bacterial infections', *Infection*, Feb. 2024, doi: 10.1007/s15010-024-02178-0.

[4] A. Pirisi, 'Phage therapy—advantages over antibiotics?', *The Lancet*, vol. 356, no. 9239, p. 1418, Oct. 2000, doi: 10.1016/S0140-6736(05)74059-9.

[5] N. N. Tran, T. Morrisette, S. C. J. Jorgensen, J. M. Orench-Benvenutti, and R. Kebriaei, 'Current therapies and challenges for the treatment of Staphylococcus aureus biofilm-related infections', *Pharmacotherapy*, vol. 43, no. 8, pp. 816–832, Aug. 2023, doi: 10.1002/phar.2806.

[6] Q. Yang, S. Le, T. Zhu, and N. Wu, 'Regulations of phage therapy across the world', *Front Microbiol*, vol. 14, p. 1250848, Oct. 2023, doi: 10.3389/fmicb.2023.1250848.

[7] S. C. Nang *et al.*, 'Pharmacokinetics/pharmacodynamics of phage therapy: a major hurdle to clinical translation', *Clin Microbiol Infect*, vol. 29, no. 6, pp. 702–709, Jun. 2023, doi: 10.1016/j.cmi.2023.01.021.

[8] 'Staphylococcus aureus in Healthcare Settings | HAI | CDC'. Accessed: Feb. 12, 2024. [Online]. Available: https://www.cdc.gov/hai/organisms/staph.html

[9] 'WHO publishes list of bacteria for which new antibiotics are urgently needed'. Accessed: Nov. 15, 2023. [Online]. Available: https://www.who.int/news/item/27-02-2017-who-publishes-list-of-bacteria-for-which-new-antibiotics-are-urgently-needed

[10] M. J. Horsburgh, J. L. Aish, I. J. White, L. Shaw, J. K. Lithgow, and S. J. Foster, 'sigmaB modulates virulence determinant expression and stress resistance: characterization of a functional rsbU strain derived from Staphylococcus aureus 8325-4', *J Bacteriol*, vol. 184, no. 19, pp. 5457–5467, Oct. 2002, doi: 10.1128/JB.184.19.5457-5467.2002.

[11] B. A. Diep *et al.*, 'Complete genome sequence of USA300, an epidemic clone of community-acquired meticillin-resistant Staphylococcus aureus', *Lancet*, vol. 367, no. 9512, pp. 731–739, Mar. 2006, doi: 10.1016/S0140-6736(06)68231-7.

[12] A. M. Kropinski, 'Practical Advice on the One-Step Growth Curve', *Methods Mol Biol*, vol. 1681, pp. 41–47, 2018, doi: 10.1007/978-1-4939-7343-9_3.

[13] T. Seemann, 'Prokka: rapid prokaryotic genome annotation', *Bioinformatics*, vol. 30, no. 14, pp. 2068–2069, Jul. 2014, doi: 10.1093/bioinformatics/btu153.

[14] D. Chae, 'Phage-host-immune system dynamics in bacteriophage therapy: basic principles and mathematical models', *Transl Clin Pharmacol*, vol. 31, no. 4, pp. 167–190, Dec. 2023, doi: 10.12793/tcp.2023.31.e17.

[15] B. J. Cairns, A. R. Timms, V. A. A. Jansen, I. F. Connerton, and R. J. H. Payne, 'Quantitative models of in vitro bacteriophage-host dynamics and their application to phage therapy', *PLoS Pathog*, vol. 5, no. 1, p. e1000253, Jan. 2009, doi: 10.1371/journal.ppat.1000253.

[16] R. J. Payne, D. Phil, and V. A. Jansen, 'Phage therapy: the peculiar kinetics of self-replicating pharmaceuticals', *Clin Pharmacol Ther*, vol. 68, no. 3, pp. 225–230, Sep. 2000, doi: 10.1067/mcp.2000.109520.

[17] R. J. H. Payne and V. A. A. Jansen, 'Pharmacokinetic principles of bacteriophage therapy', *Clin Pharmacokinet*, vol. 42, no. 4, pp. 315–325, 2003, doi: 10.2165/00003088-200342040-00002.

[18] C. Y. (Joey) Leung and J. S. Weitz, 'Modeling the synergistic elimination of bacteria by phage and the innate immune system', *Journal of Theoretical Biology*, vol. 429, pp. 241–252, Sep. 2017, doi: 10.1016/j.jtbi.2017.06.037.

[19] T. Bigwood, J. A. Hudson, and C. Billington, 'Influence of host and bacteriophage concentrations on the inactivation of food-borne pathogenic bacteria by two phages', *FEMS Microbiol Lett*, vol. 291, no. 1, pp. 59–64, Feb. 2009, doi: 10.1111/j.1574-6968.2008.01435.x.

[20] J. M. Obeso, P. García, B. Martínez, F. N. Arroyo-López, A. Garrido-Fernández, and A. Rodriguez, 'Use of Logistic Regression for Prediction of the Fate of Staphylococcus aureus in Pasteurized Milk in the Presence of Two Lytic Phages', *Applied and Environmental Microbiology*, vol. 76, no. 18, pp. 6038–6046, Sep. 2010, doi: 10.1128/AEM.00613-10.

[21] R. J. Payne and V. A. Jansen, 'Understanding bacteriophage therapy as a density-dependent kinetic process', *J Theor Biol*, vol. 208, no. 1, pp. 37–48, Jan. 2001, doi: 10.1006/jtbi.2000.2198.

[22] A. A. Schmalstig, S. Freidy, P. O. Hanafin, M. Braunstein, and G. G. Rao, 'Reapproaching Old Treatments: Considerations for PK/PD Studies on Phage Therapy for Bacterial Respiratory

Infections', *Clin Pharmacol Ther*, vol. 109, no. 6, pp. 1443–1456, Jun. 2021, doi: 10.1002/cpt.2214.

[23] L. M. Kasman, A. Kasman, C. Westwater, J. Dolan, M. G. Schmidt, and J. S. Norris, 'Overcoming the Phage Replication Threshold: a Mathematical Model with Implications for Phage Therapy', *J Virol*, vol. 76, no. 11, pp. 5557–5564, Jun. 2002, doi: 10.1128/JVI.76.11.5557-5564.2002.

[24] S. T. Abedon, 'Phage therapy dosing: The problem(s) with multiplicity of infection (MOI)', *Bacteriophage*, vol. 6, no. 3, p. e1220348, Aug. 2016, doi: 10.1080/21597081.2016.1220348.

[25] S. M. Lehman *et al.*, 'Design and Preclinical Development of a Phage Product for the Treatment of Antibiotic-Resistant Staphylococcus aureus Infections', *Viruses*, vol. 11, no. 1, Art. no. 1, Jan. 2019, doi: 10.3390/v11010088.

[26] R. Capparelli, M. Parlato, G. Borriello, P. Salvatore, and D. Iannelli, 'Experimental Phage Therapy against Staphylococcus aureus in Mice', *Antimicrobial Agents and Chemotherapy*, vol. 51, no. 8, pp. 2765–2773, Aug. 2007, doi: 10.1128/aac.01513-06.

[27] A. Leprince and J. Mahillon, 'Phage Adsorption to Gram-Positive Bacteria', *Viruses*, vol. 15, no. 1, p. 196, Jan. 2023, doi: 10.3390/v15010196.

[28] J. Bertozzi Silva, Z. Storms, and D. Sauvageau, 'Host receptors for bacteriophage adsorption', *FEMS Microbiol Lett*, vol. 363, no. 4, p. fnw002, Feb. 2016, doi: 10.1093/femsle/fnw002.

[29] B. R. Levin and J. J. Bull, 'Population and evolutionary dynamics of phage therapy', *Nat Rev Microbiol*, vol. 2, no. 2, pp. 166–173, Feb. 2004, doi: 10.1038/nrmicro822.

[30] D. T. Kysela and P. E. Turner, 'Optimal bacteriophage mutation rates for phage therapy', *J Theor Biol*, vol. 249, no. 3, pp. 411–421, Dec. 2007, doi: 10.1016/j.jtbi.2007.08.007.

[31] A. Rabinovitch, I. Aviram, and A. Zaritsky, 'Bacterial debris-an ecological mechanism for coexistence of bacteria and their viruses', *J Theor Biol*, vol. 224, no. 3, pp. 377–383, Oct. 2003, doi: 10.1016/s0022-5193(03)00174-7.

[32] 'Alternative stable states in host–phage dynamics | Theoretical Ecology'. Accessed: Feb. 27, 2024. [Online]. Available: https://link.springer.com/article/10.1007/s12080-007-0001-1

Table 1. Parameter estimates of the phage-bacteria co-dynamics for S. aureus SH1000 / V1SA019

	Parameter	Value	Relative standard error (%)	Bootstrap estimates		
				P2.5	Median	P97.5
Fixed effects[a]	alpha (h^{-1})	1.64	1.91	1.45	1.62	1.70
	Bmax (CFU/mL)	1.32E+10	NA (fixed)	NA	NA	NA
	mut (h-1)	2.64E-09	44.2	6.97E-10	2.56E-09	1.25E-08
	$bind_S$ (h-1)	2.45E-09	8.6	1.34E-09	2.30E-09	3.31E-09
	$bind_R$ (h-1)	4.47E-11	7.6	1.94E-11	3.86E-11	5.75E-11
	lysis (h-1)	6.98	9.9	5.53343	7.16135	9.64491
	burst (PFU/mL)	179	22.4	102.83	203.832	692.648
	dec (h-1)	0.0177	13.6	0.0111	0.0186	0.0248
Random effects[b]	omega_alpha	0.043 (4.3%)	35.2	0.017	0.034	0.117
	omega_mut	1.49 (286%)	29.1	0.75	1.45	2.28
	omega_$bind_S$	0.335 (34%)	48.6	0.126	0.368	0.823
	omega_$bind_R$	0.151 (15%)	43.0	0.0995	0.231	0.686
	omega_lysis	0.398 (41%)	17.8	0.274	0.409	0.564
	omega_burst	0.861 (105%)	17.5	0.471	0.893	1.262
	omega_dec	0.442 (46%)	28.6	0.193	0.369	0.651
Error model parameters[c]	a(B)	0.548 (4.52%)	4.52	0.476	0.546	0.622
	a(V)	0.11 (14.3%)	14.3	0.059	0.107	0.173
	b(V)	0.0553 (6.61%)	6.61	0.0345	0.0537	0.0680
Others[d]	$Prolif_S$ (CFU/mL)	4.8E+04 (54.8%)	NA	NA	NA	NA
	$Inund_S$ (PFU/mL)	6.8E+08 (14.6%)	NA	NA	NA	NA
	$Prolif_R$ (CFU/mL)	2.67E+06 (69.1%)	NA	NA	NA	NA
	$Inund_R$ (PFU/mL)	3.68E+10 (3.3%)	NA	NA	NA	NA

[a]Fixed effect parameters are as described in the main text.

[b] Omega parameters are expressed as standard deviations of random effects along with coefficient of variation of the corresponding parameter within brackets

[c] Error model parameters are as follows: a(B), coefficient of additive error of bacteria count, a(V) and b(V), coefficient of additive and proportional error of phage count, respectively.

[d] Proliferation and inundation threshold values are given as mean (CV%) of Bayesian posterior estimates from each experiment.

Table S1. Adsorption time and Maximum adsorption time. A: Adsorption time and B: Maximum adsorption time determined for phages V1SA019, V1SA020, V1SA022 on strains SH1000 and USA300. nd : not determined.

A.

Adsorption time (min)		Bacterial strains	
		SH1000	**USA300**
Phages	**V1SA019**	8	8
	V1SA020	20	nd
	V1SA022	16	nd

B.

Maximum adsorption time (min)		Bacterial strains	
		SH1000	**USA300**
Phages	**V1SA019**	24	32
	V1SA020	32	nd
	V1SA022	24	nd

Table S2. Burst size values determined for phages V1SA019, V1SA020, V1SA022 on strains SH1000 and USA300. Calculation based on data from One-Step-Growth-Curve experiment. nd : not determined.

Burst size values		Bacterial strains	
		SH1000	**USA300**
Phages	**V1SA019**	42	134
	V1SA020	24	nd
	V1SA022	27	nd

Table S3. Comparison of parameters of the phage-bacteria co-dynamics for the 3 other bacteria/phage pairs.

		SH1000 / V1SA019	**SH1000 / V1SA020**	**SH1000 / V1SA022**	**USA300 / V1SA019**
Fixed effects[a]	alpha (h^{-1})	1.64 (1.91%)	1.33 (3.92%)	1.31 (3.29%)	1.8 (2.66%)
	Bmax (CFU/mL)	1.32E+10 (NA, fixed)	1.9E+10 (43.7%)	2.72E+10 (30.9%)	5.23e+08 (32.5%)
	mut (h-1)	2.64E-09 (44.2%)	1.46E-10 (382%)	6.85E-13 (>200%)	1.26e-13 (>200%)
	$bind_S$ (h-1)	2.45E-09 (8.6%)	6.19e-09 (22%)	2.74E-09 (21.2%)	1.7e-08 (12.6%)
	$bind_R$ (h-1)	4.47E-11 7.6%)	5.65e-11 (14.6%)	1.09E-11 (42.4%)	4.82e-10 (33.5%)
	lysis (h-1)	6.98 59.9%)	4.37 (8.13%)	5.96 (13.6%)	6.29 (12.7%)
	burst (PFU/mL)	179 (22.4%)	139 45.6%)	503 (35%)	17.9 (33.9%)

		SH1000 / V1SA019	SH1000 / V1SA020	SH1000 / V1SA022	USA300 / V1SA019
	dec (h-1)	0.0177 (13.6%)	0.0336 (18.6%)	0.0499 (16.7%)	0.0109 (45.7%)
Random effects[b]	omega_alpha	0.043 (35.2%)	0.207 (11.8%)	0.172 (11.6%)	0.108 (24.8%)
	Omega_Bmax	NA	0.82 (40.2%)	0.754 (32%)	1.63 (14%)
	omega_mut	1.49 (29.1%)	2.57 (46.8%)	4.59 (28.4%)	7.62 (29.7%)
	omega_$bind_S$	0.335 (48.6%)	1.17 (15.8%)	1.35 (14.5%)	0.604 (18.4%)
	omega_$bind_R$	0.151 (43.0%)	0.243 (27.9%)	0.745 (38.2%)	0.962 (33.1%)
	omega_lysis	0.398 (17.8%)	0.427 (15.1%)	0.634 (17.6%)	0.599 (27%)
	omega_burst	0.861 (17.5%)	0.963 (17.1%)	1.25 (21.9%)	1.48 (13.8%)
	omega_dec	0.442 (28.6%)	0.53 (29.1%)	0.492 (33%)	1.41 (21.5%)
	Correlation	NA	$Bind_S$ alpha -0.751 (14.3%)	NA	NA
Error model parameters[c]	a(B)	0.548	0.6	0.575	0.824
	a(V)	0.11	0.38	0.319	0.168
	b(V)	0.0553	NA	NA	0.0475
Others[d]	$Prolif_S$ (CFU/mL)	4.8E+04 (54.8%)	7.00E+04 (174.9%)	4.78E+04 (63.8%)	2.12E+05 (350.5%)
	$Inund_S$ (PFU/mL)	6.8E+08 (14.6%)	2.95E+08 (74.7%)	6.21E+08 (64.5%)	1.11E+08 (36.5%)
	$Prolif_R$ (CFU/mL)	2.67E+06 (69.1%)	6.19E+06 (121.7%)	1.50E+07 (173.7%)	9.64E+06 (598.4%)
	$Inund_R$ (PFU/mL)	3.68E+10 (3.3%)	2.40E+10 (18.1%)	1.19E+11 (24.7%)	3.76E+09 (33.1%)

[a]Fixed effect parameters are as described in the main text and expressed as population estimate (relative standard error).

[b] Omega parameters are expressed as standard deviations of random effects (relative standard errors)

[c] Error model parameters are as follows: a(B), coefficient of additive error of bacteria count, a(V) and b(V), coefficient of additive and proportional error of phage count, respectively.

[d] Proliferation and inundation threshold values are given as mean (CV%) of Bayesian posterior estimates from each experiment.

Table S4. List of mutated genes in SH1000 after 24 hours of exposure to phage V1SA019. In bold: genes involved in the teichoic acid biosynthesis pathway.

MOI	Mutant	Gene	Effect
0.01	KR19	**tarK**	missense_variant c.536A>G p.His179Arg
		tarA	missense_variant c.665G>T p.Arg222Ile
		purR	missense_variant c.286C>T p.Arg96Cys
	KR20	S35	intragenic_variant n.508155A>G
		tarK	missense_variant c.536A>G p.His179Arg
		tsr24	non_coding_transcript_variant
		tarA	missense_variant c.665G>T p.Arg222Ile
		znuB	missense_variant c.143G>A p.Ser48Asn
	KR21	tsr24	non_coding_transcript_variant
		tarA	missense_variant c.665G>T p.Arg222Ile
1	KR25	tsr24	non_coding_transcript_variant
		rpoB	missense_variant c.2161A>G p.Thr721Ala
		rfe/tagO	frameshift_variant&missense_variant c.556delGinsAT p.Val186fs
	KR26	S35	intragenic_variant n.508155A>G
		tsr24	non_coding_transcript_variant
		mrcB	disruptive_inframe_insertion c.785_787dupGCA p.Arg262_Ile263insSer
		tarA	missense_variant c.665G>T p.Arg222Ile
	KR27	mrcB	missense_variant c.691C>T p.Pro231Ser
		tarA	missense_variant c.665G>T p.Arg222Ile
100	KR31	**rfe/tagO**	deletion of 823 nucleotides
	KR32	**tarK**	missense_variant c.536A>G p.His179Arg
		rfe/tagO	frameshift_variant c.853delG p.Val285fs
	KR33	**tarK**	missense_variant c.536A>G p.His179Arg
		rfe/tagO	frameshift_variant c.853delG p.Val285fs

Table S5. Apparition of SH1000 resistant mutants to V1SA019 over time of kinetic according to MOI. Nd : not determined.

Resistants to V1SA019 (total tested)		Time of kinetic				
		8 hrs	**10 hrs**	**12 hrs**	**14 hrs**	**24 hrs**
MOI	**0.01**	0 (30)	0 (30)	0 (30)	1 (3)	23 (24)
	1	1 (15)	0 (1)	0 (22)	10 (10)	30 (30)
	100	2 (30)	5 (27)	nd	nd	30 (30)

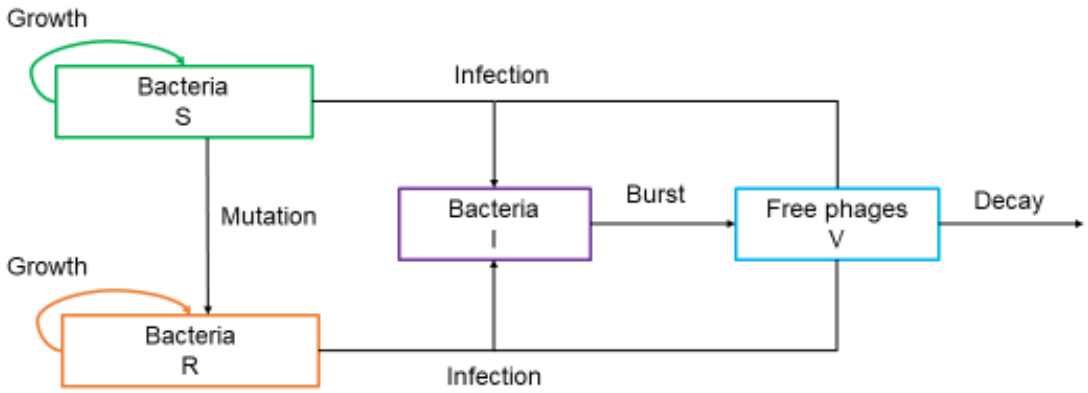

Figure 1. Structural model of the bacteria – phage codynamics

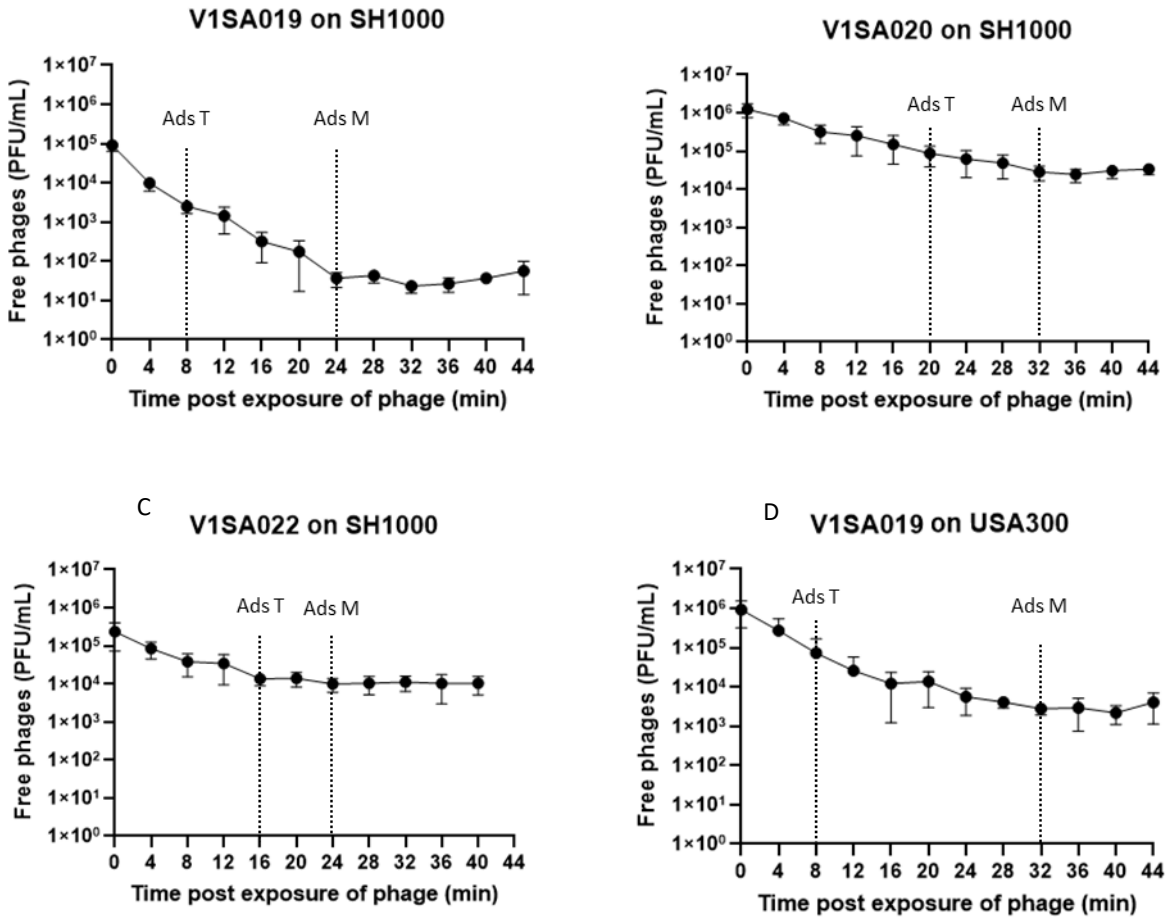

Figure 2. Adsorption kinetics for V1SA019 (A), V1SA020 (B), V1SA022 (C) phages on SH1000 strain and V1SA019 (D) on USA300 strain. Each circle represents the average of 3 independent experiments with standard deviation. Ads T: Adsorption time (min). Ads M: Maximum adsorption time (min).

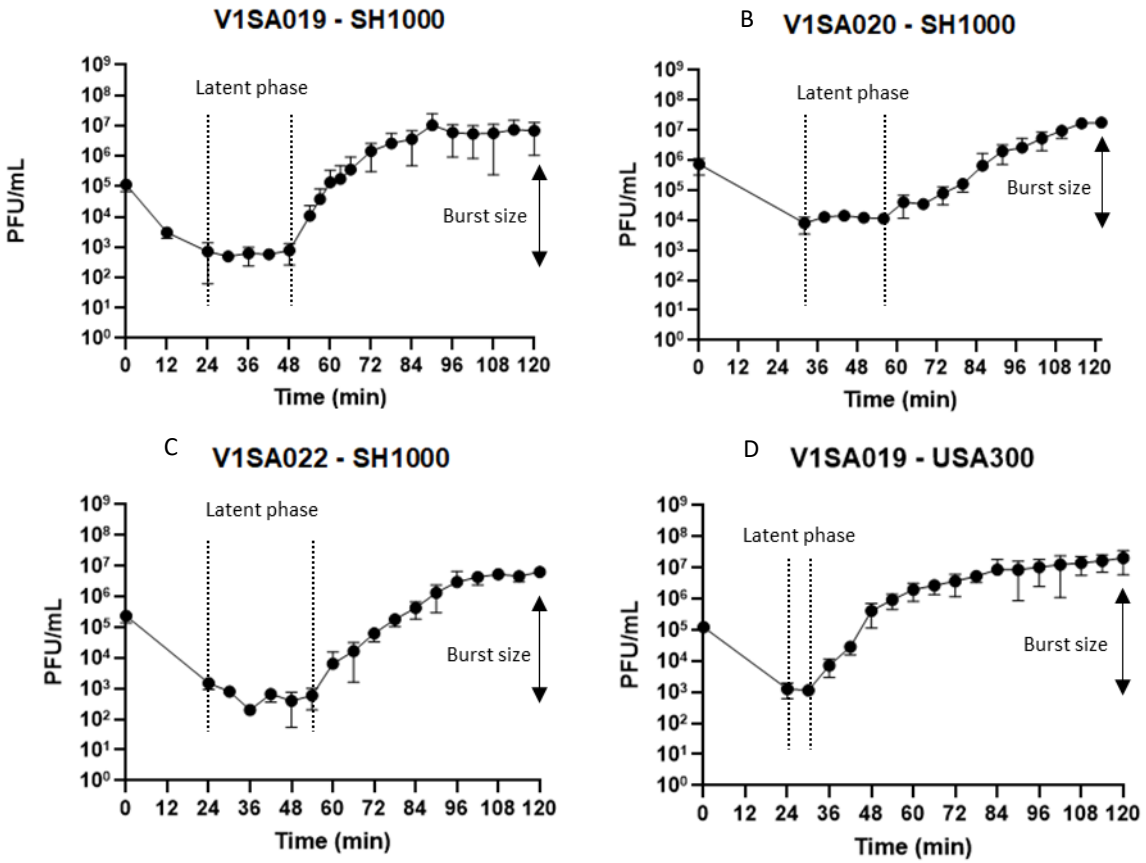

Figure 3. One-Step-Growth-Curve (for burst size value calculation) for V1SA019 (A), V1SA020 (B), V1SA022 (C) phages on SH1000 strain and V1SA019 (D) on USA300 strain. Each circle represents the average of 3 independent experiments with standard deviation. The latent phase is indicated between the dotted lines. The solid arrow represents the burst size.

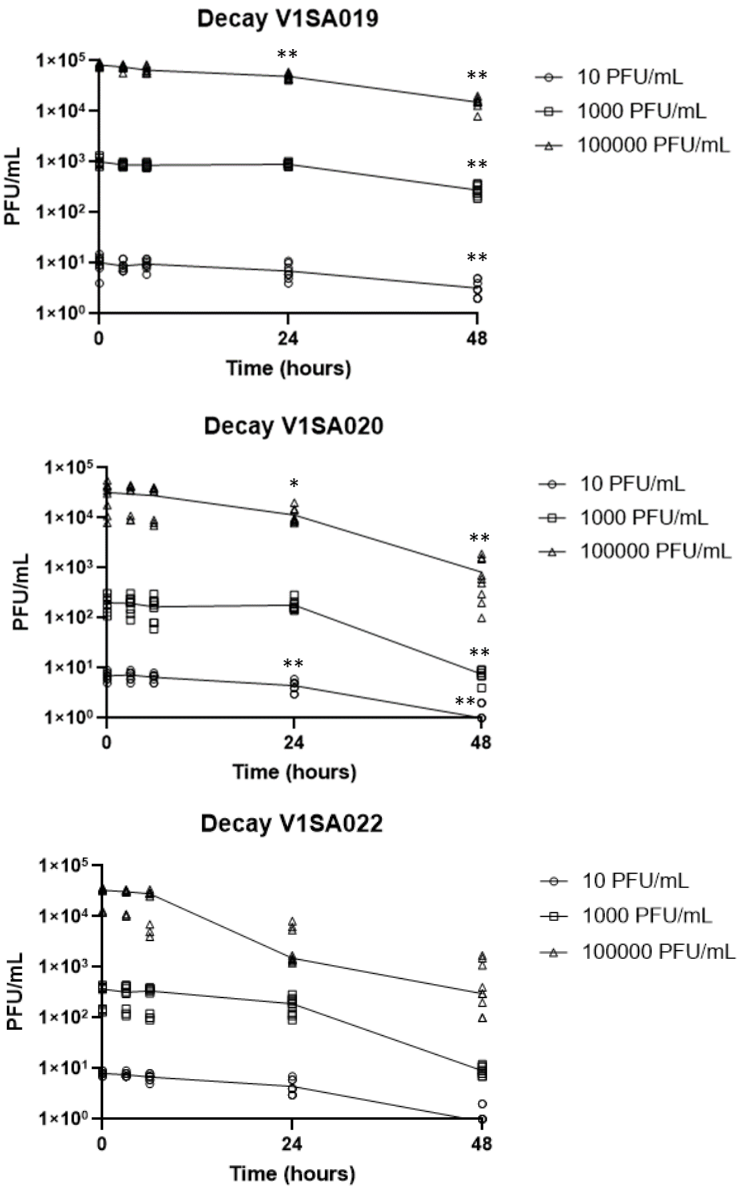

Figure 4. Phage decay of V1SA019, V1SA020, V1SA022. Each symbol represents an experimental point. Connecting line represents the median. Statistical analysis compared two time points via wilcoxon matched pairs signed rank test. *: p-value < 0.05; **: p-value < 0.005.

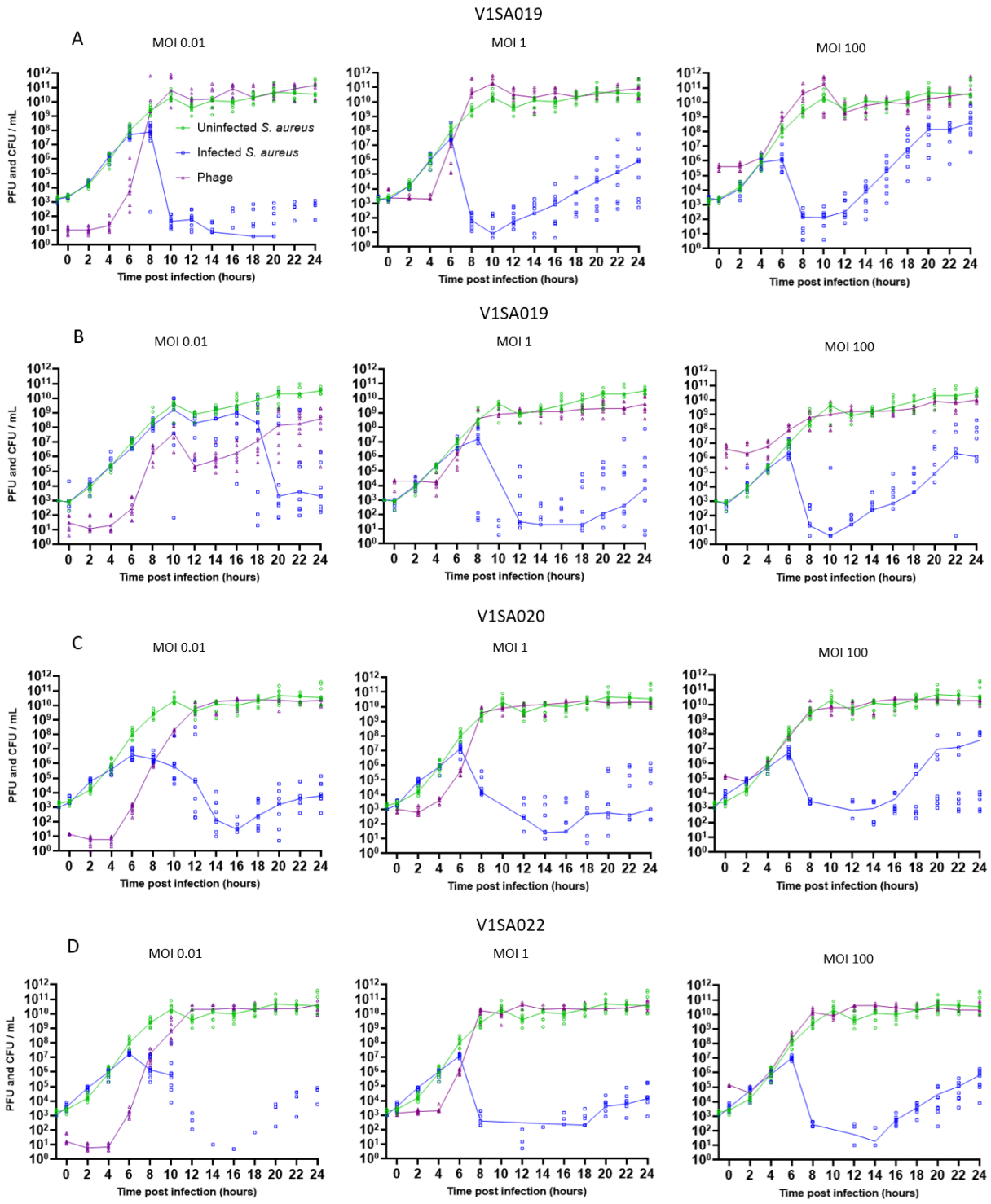

Figure 5. in vitro time-kill experiments between V1SA019 and SH1000(A) or USA300 (B), V1SA020 and SH1000 (C), V1SA022 and SH1000 (D). Each symbol represents an experimental point. Connecting line represents the median. Green: Enumeration of S. *aureus* in absence of phage (control condition). Blue: Enumeration of S. *aureus* in the presence of phage. Purple: Free phages in the presence of S. *aureus*.

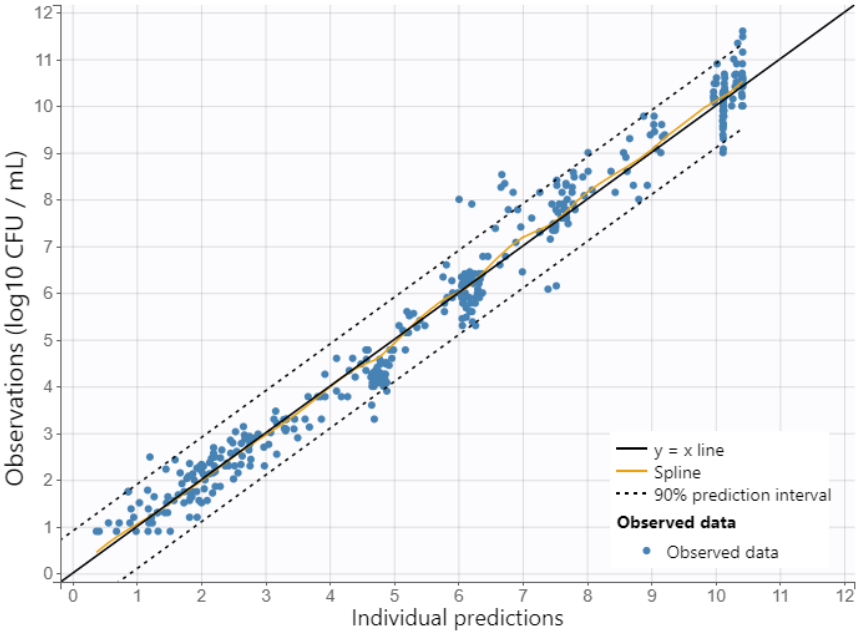

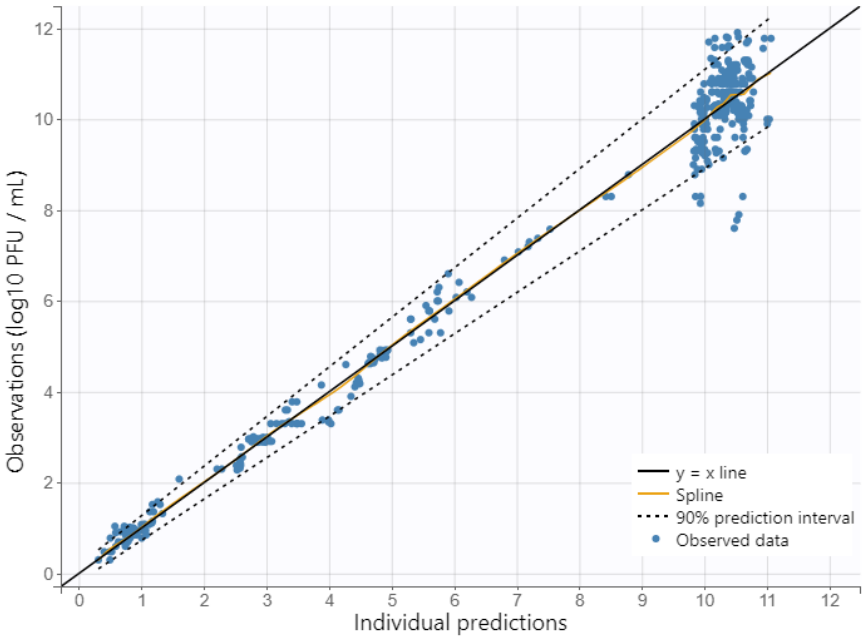

Figure 6. Observations versus model-based predictions of bacteria (top) and phage (bottom) counts for the V1SA019 / SH1000 pair.
The blue dots indicate observation-prediction pairs. The black solid line is the y = x line, the yellow line is the spline regression line. The dashed lines indicate the 90% prediction interval.

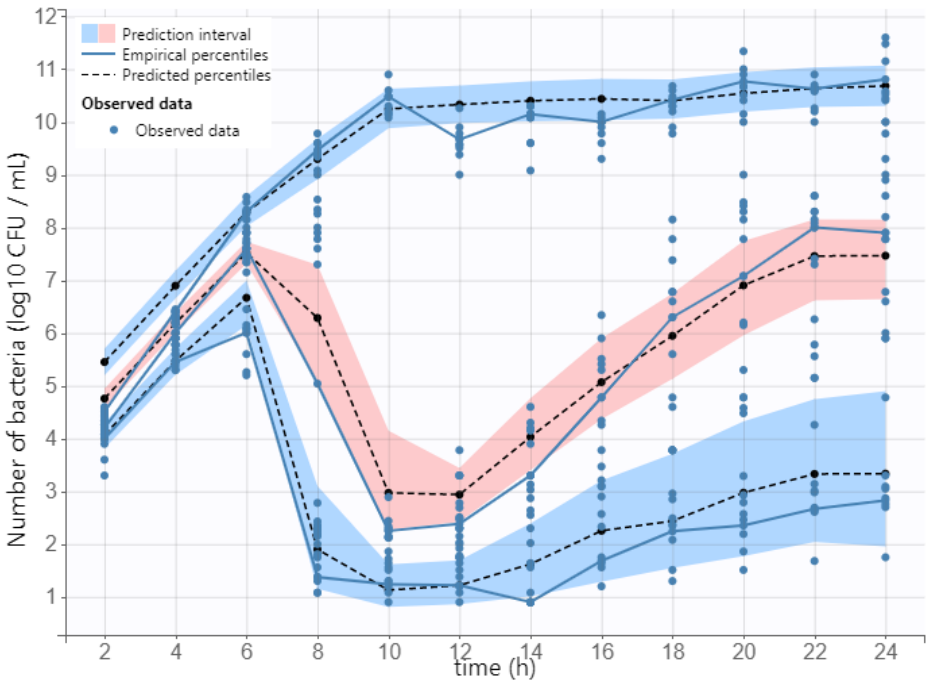

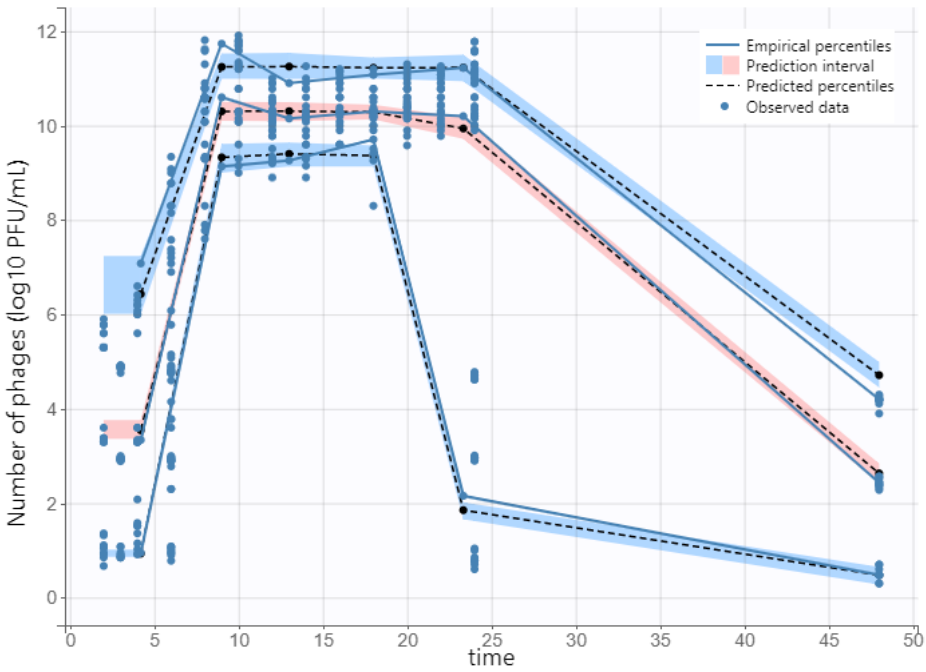

Figure 7. Visual predictive checks obtained with the final model for the V1SA019 / SH1000 pair.

Top and bottom panel show VPC for bacteria and phage, respectively. Blue dots are observed data. Blue solid and black dashed lines are 10th, 50th (median) and 90th percentiles of observed and simulated data (n = 1000 for each experiment), respectively. Blue and pink colored areas are 90% prediction intervals of corresponding simulated percentiles.

A

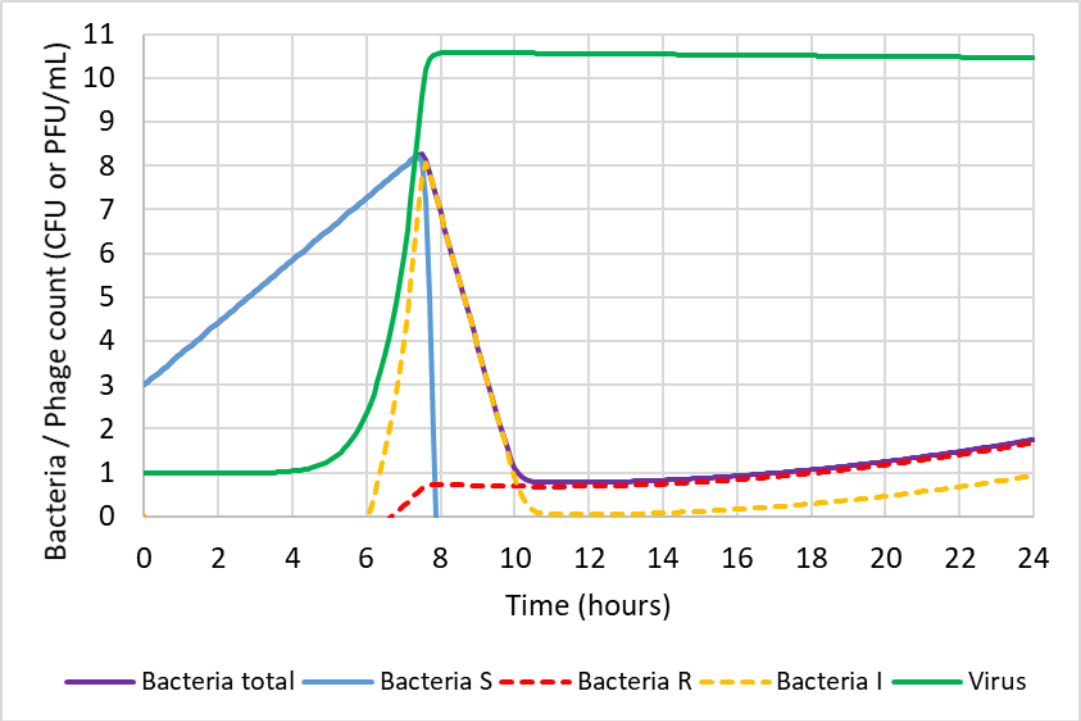
Bacteria / Phage count (CFU or PFU/mL)
11
10
9
8
7
6
5
4
3
2
1
0
0
2
4
6
8
10
12
14
16
18
20
22
24
Time (hours)
Bacteria total
Bacteria S
Bacteria R
Bacteria I
Virus

B

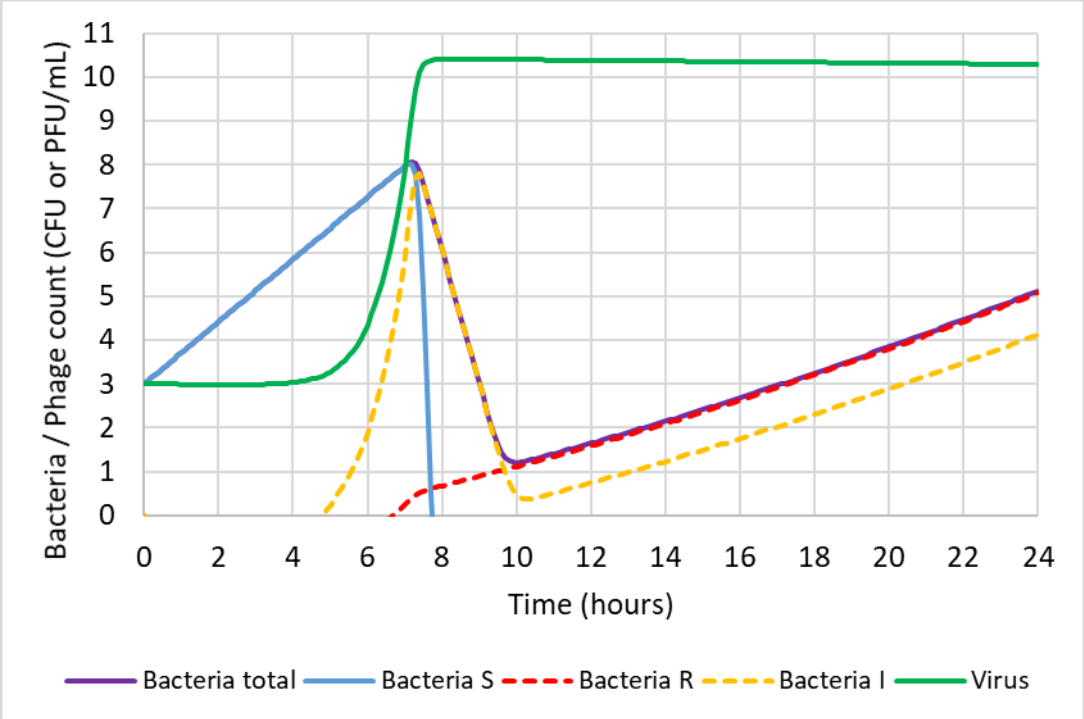
Bacteria / Phage count (CFU or PFU/mL)
11
10
9
8
7
6
5
4
3
2
1
0
0
2
4
6
8
10
12
14
16
18
20
22
24
Time (hours)
Bacteria total
Bacteria S
Bacteria R
Bacteria I
Virus

C

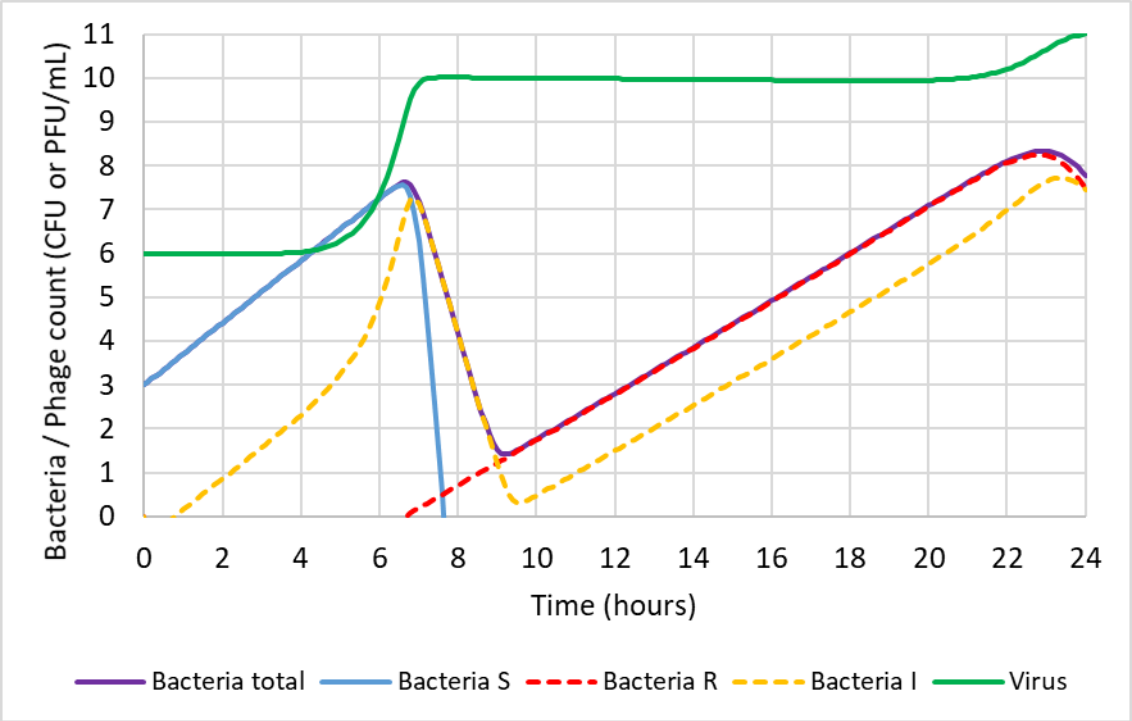

D

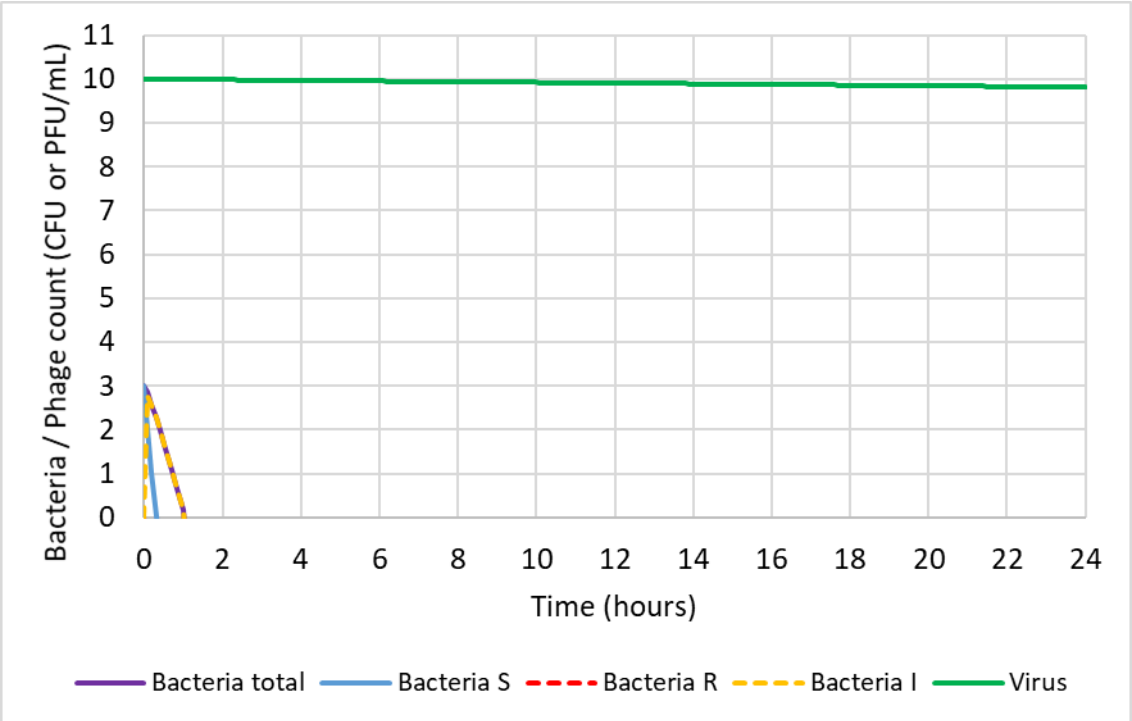

Figure 8. Simulated dynamics of bacteria and phage
Simulations were performed with typical parameter values of the final model for V1SA019 / SH1000 reported in

Table **1**. Initial number of susceptible bacteria is 10^3 in all simulations. Initial number of phages is 10, 10^3, 10^6 and 10^{10} in panel A, B, C, and D, respectively.

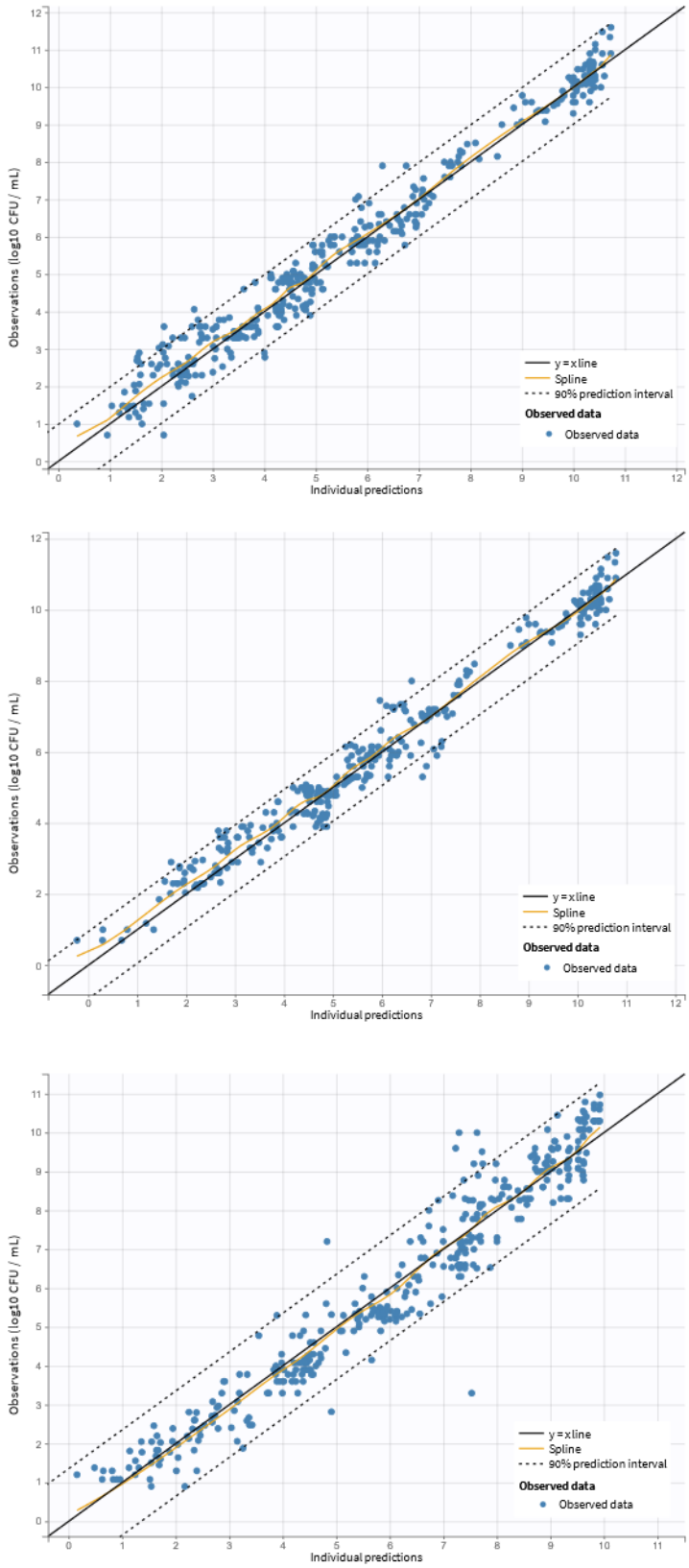

Supplementary figure S1. Observations versus model predictions of bacteria count

Top, middle and bottom panel are bacteria counts for V1SA020 / SH1000, V1SA022 / SH1000, and V1SA019 / USA 300 pairs, respectively.

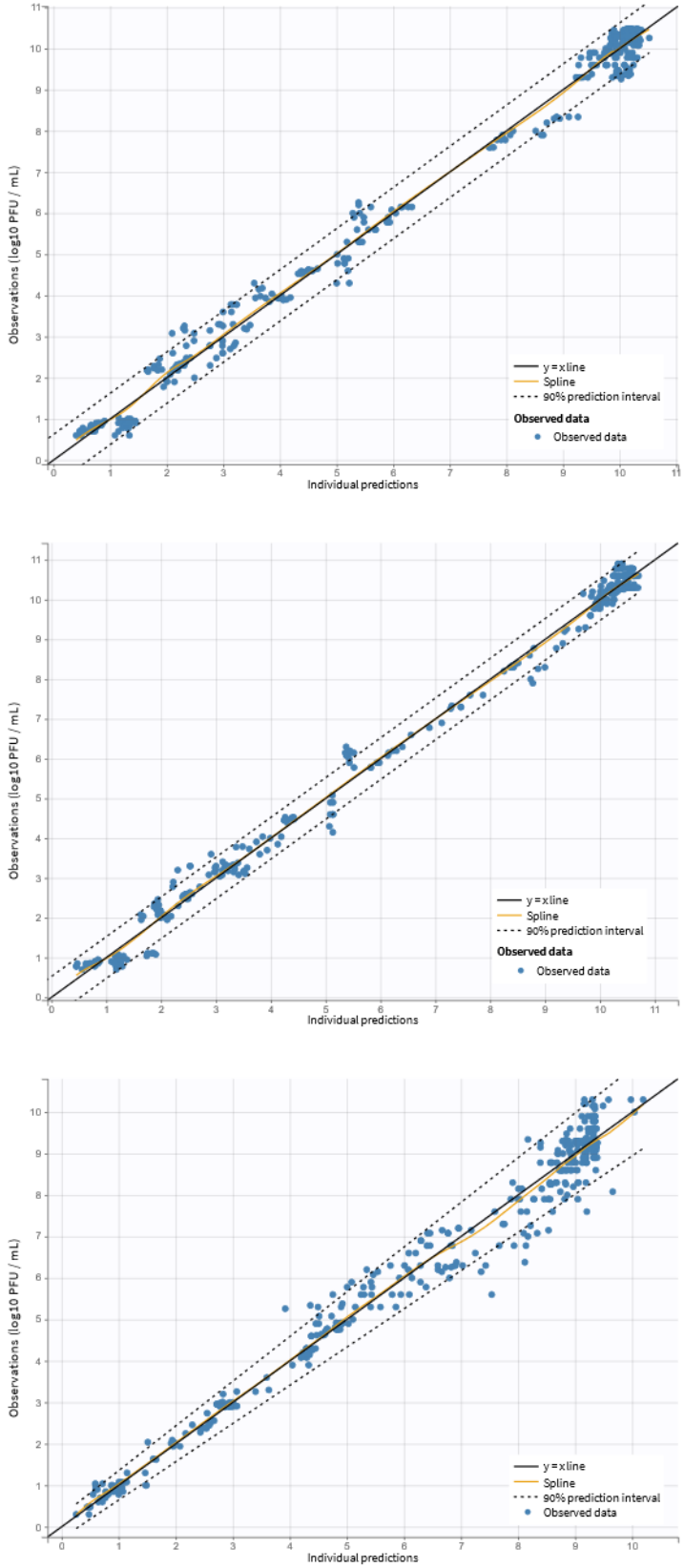

Supplementary figure S2. Observations versus model predictions of phage count

Top, middle and bottom panel are phage counts for V1SA020 / SH1000, V1SA022 / SH1000, and V1SA019 / USA 300 pairs, respectively.

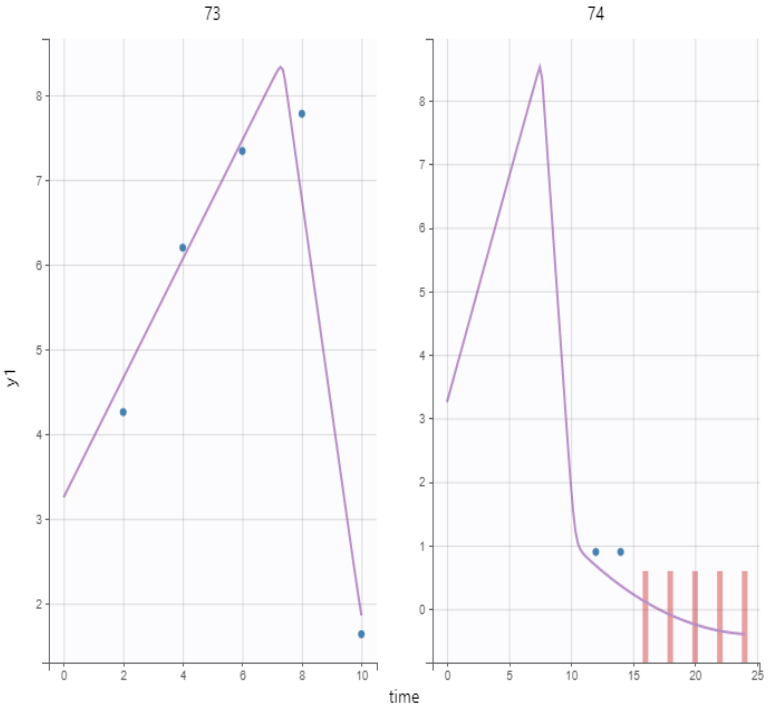

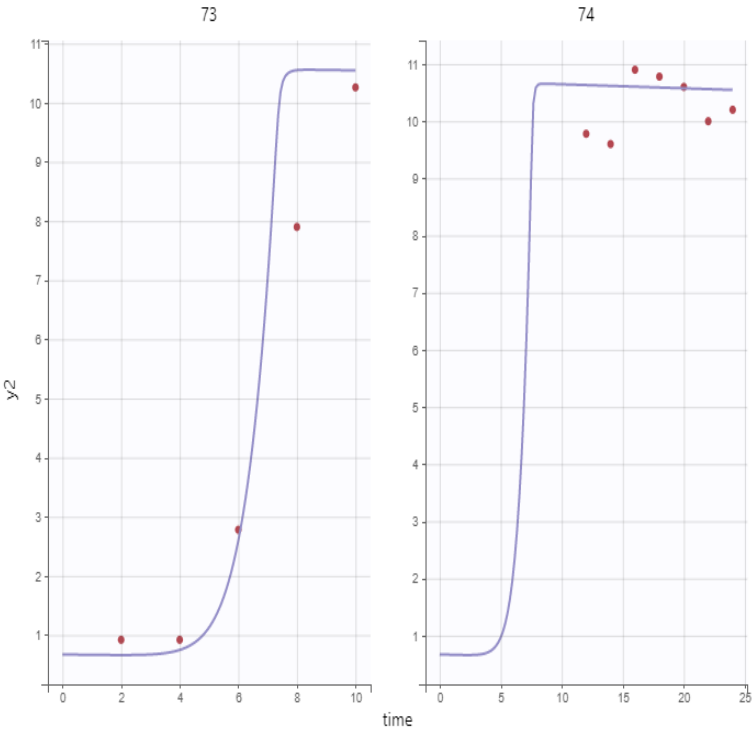

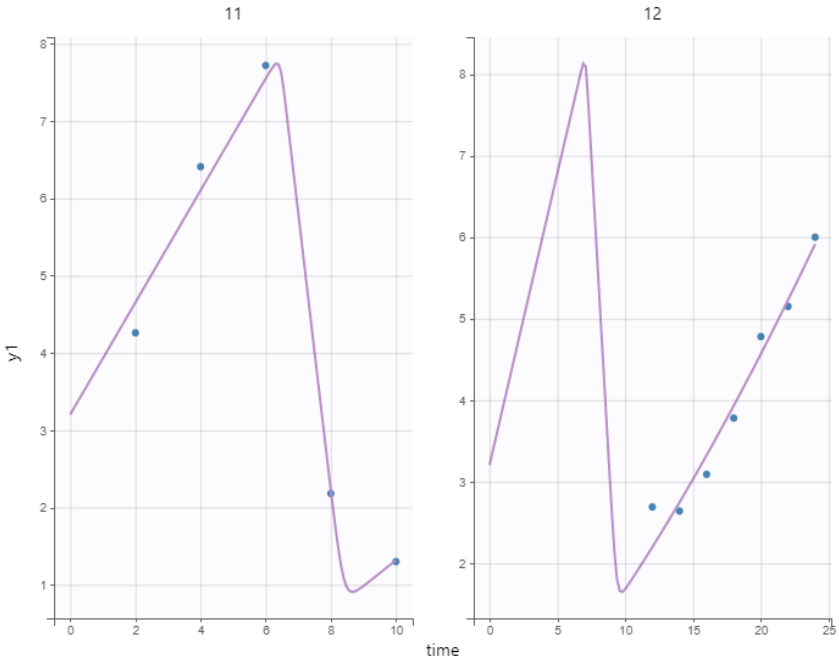
11
12
y1
time

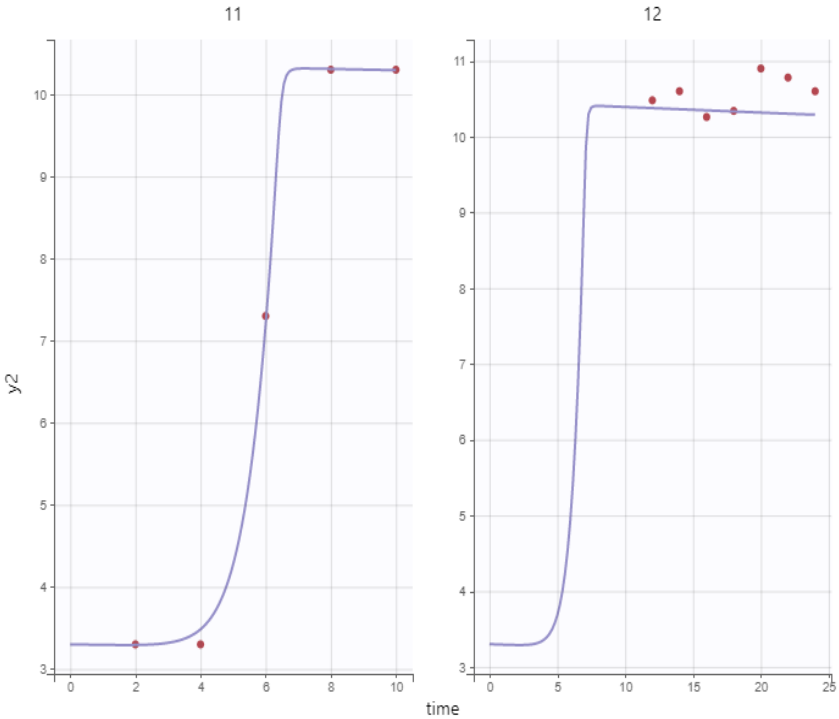
11
12
y2
time

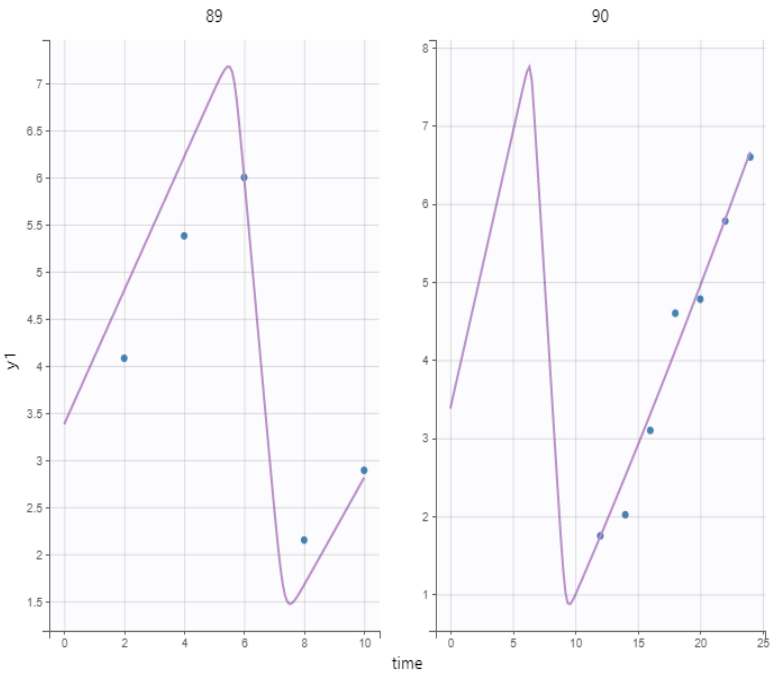

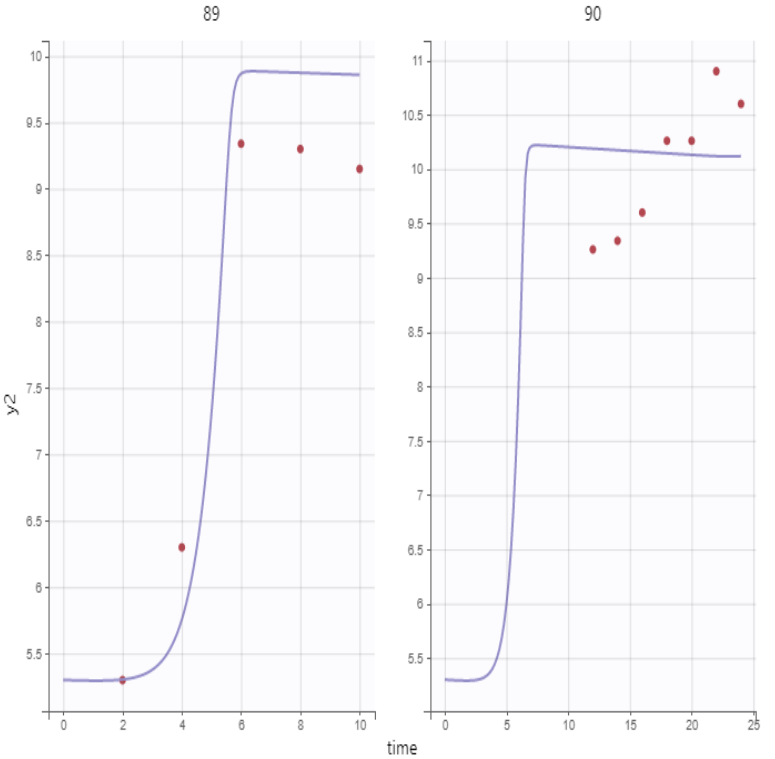

Figure S3. Examples of individual fits of bacteria and phage counts for the V1SA19 / SH1000 model

Blue and red dots are bacteria (y1) and phage (y2) counts, respectively. Pink and purple lines are individual model predictions for bacteria and phage, respectively. Red bars indicate observations below the quantification limit.

#73 and 74: B(0) = 1.8E03; V(0) = 5.0E00; MOI initial ≈ 0.01

#11 and 12: B(0) = 1.6E03; V(0) = 2.0E03; MOI initial ≈ 1

#89 and 90: B(0) = 2.4E03; V(0) = 2.0E05; MOI initial ≈ 100

Each pair represents two successive experiments with the same initial conditions and different time windows, 1-10h and 12-24h.